Study of Efficient Plasma Production in Inductively Coupled Plasma

Takagi, Kenichi
Department of Electronic Device Engineering, Graduate School of Information Science and Electrical Engineering, Kyushu University

Kuroki, Yukinori
Department of Electronic Device Engineering, Graduate School of Information Science and Electrical Engineering, Kyushu University

Study of Efficient Plasma Production in Inductively Coupled Plasma

Ken-ichi TAKAGI* and Yukinori KUROKI*

Abstract: We have examined an Inductively coupled plasma (ICP) production mechanism for the different types of the antenna by means of a Langmuir probe method, an electrical measurement of an antenna and an induction field measurement. We could find that the plasma production depends on the antenna geometry. Especially the important factors are given in the following, the capacitance between the antenna and the plasma, the phase angle of the induction field for the antenna voltage and the induction field penetration into the plasma. These factors arise from the heated electron loss at the quartz window. It is proved that the plasma production efficiency rises due to the magnetic field to control the electron loss.

Keywords: Inductively coupled plasma, Plasma, Production efficiency, Induction field, Capacitively coupling

1. Introduction

Recently, ICP source have been applying widely to the material plasma processing, to meet a demand for the high throughput and so on. ICP source is characterized by the simple structure and more efficient plasma production than that of capacitively coupled plasma, which has been used widely up to the present. To draw the potentiality of the ICP source, it is important to understand the plasma production mechanism.

To understand the plasma production efficiency physically, we have investigated the ICP production mechanism for the different types of the single loop antenna[1]-[5], which has the different facing area to the plasma. The plasma production efficiency depends on the antenna geometry. To make clear the difference of the ICP production mechanism, we made some experiments, the electrical property measurement of the antenna[2],[3], an induction field profile measurement[5], and the Langmuir probe measurement with and without a weak DC magnetic field[2],[4]. We arrived at the conclusion that the plasma production efficiency depended on the heated electron loss at the quartz window. In this paper, we will show the summary about these experimental results

2. Experimental Setup

I will give an outline of the experimental setup briefly. For the details of the following experimental setup, see references[1]-[5]. We used a cylindrical
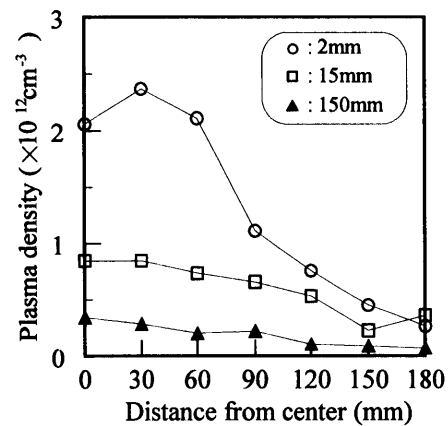

Fig.1 Plasma density dependence on antenna geometry (266mm inner diameter) (Discharge power:2000W, Gas:Ar, Pressure:1.3Pa, Measurement position:in evacuated vessel)[1]

quartz tube for the discharge power (13.56MHz) introduction to the plasma. A single loop antenna was arranged coaxially to the quartz window and supplied a discharge power toward the discharge vessel via a π type-matching network.

3. Results and Discussion

3.1 Plasma Production Efficiency

We measured the plasma density dependence on the antenna geometry as shown in **Fig.1**[1],[2]. The plasma density was inversely proportional to the antenna facing area toward the plasma. The electrostatic capacitance between the plasma and the antenna is calculated in the following equation,

$$C_{p-a} = \frac{\varepsilon S}{r} \tag{1}$$

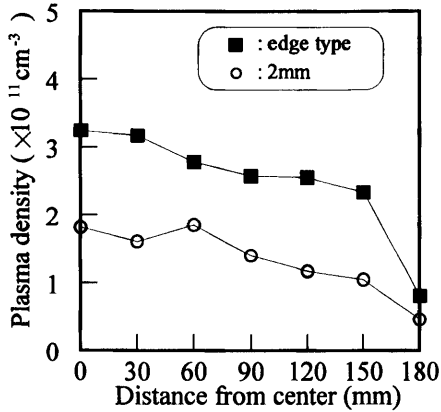* Department of Electronic Device Engineering

Fig.2 Plasma density distribution dependence on antenna geometry using discharge vessel(362mm inner diameter) (Discharge power:1000W, Gas:Ar, Pressure:1.3Pa, Measurement position:in evacuated vessel) [2],[3]

where C_{p-a} is the capacitance between the plasma and the antenna, r is the distance between the plasma and the nearest antenna side and S is the nearest antenna area to the plasma.

C_{p-a} is mainly decided by the nearest area of the antenna to the plasma. Therefore, it is suggested that the pure inductive coupling was realized by C_{p-a} decrease in the plasma production mechanism. When we made the inner side of the 2mm wide antenna to be sharpened like an edge knife, this suggestion was proved clearly as shown in **Fig.2**. We need to consider the edge effect for the antenna with small C_{p-a}.

3.2 Electric Property on Antenna

We measured the antenna current and the voltage to estimate the antenna electric property[1]-[3]. **Fig.3** shows the peak-peak voltage at the both power feed points of 2 mm wide antenna. (a) is at the Load side and (b) is at the Tune side. The electrical component for each antenna was estimated on the basis of the results. The phase angles (θ_n) at each side are estimated by using the fundamental waveforms extracted by the Fourier expansion, and the suffix n are 2, 15 and 150 to the 2mm wide, the 15mm wide and the 150mm wide antenna, respectively. The phase differences $(\Delta\theta_n)$ for each antenna are summarized in **Fig.4** . These examinations show that $\Delta\theta_n$ depends on the antenna geometry. The electrical component for the 2mm wide antenna is close to a pure inductance, for $\Delta\theta_2$ changes as a function of the azimuthal angle from the Load side to the Tune side by 90 degree. On the other
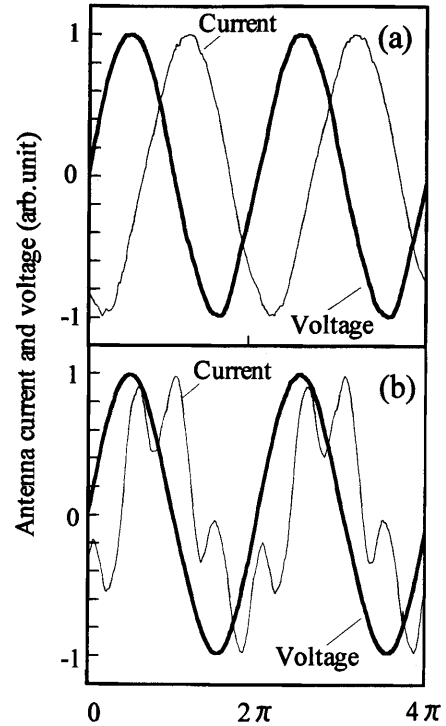

Fig.3 I-V properties at power feed points of 2 mm wide antenna (Discharge power:1000W, Gas:O_2, Pressure:1.3Pa), (a):at Load side, (b):at Tune side [2],[3]
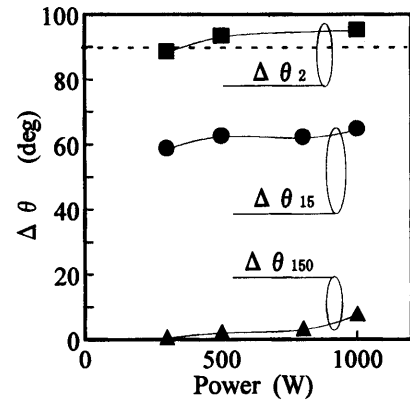

Fig.4 Phase difference($\Delta\theta_n$) dependence on the antenna geometry (Gas:O_2, Pressure:1.3Pa) [2],[3]

hand, $\Delta\theta_{150}$ is less than 10 degree and does not change grossly. We verified this result by an equivalent circuit model as shown in **Fig.5**. C_{p-a} and M are a capacitance and a mutual inductance between the antenna and the plasma respectively, L is an antenna inductance, R_a is an antenna resistance and R_p is a plasma resistance. The impedance(Z) between the both feed points for this equivalent circuit can be expressed by the following equation,
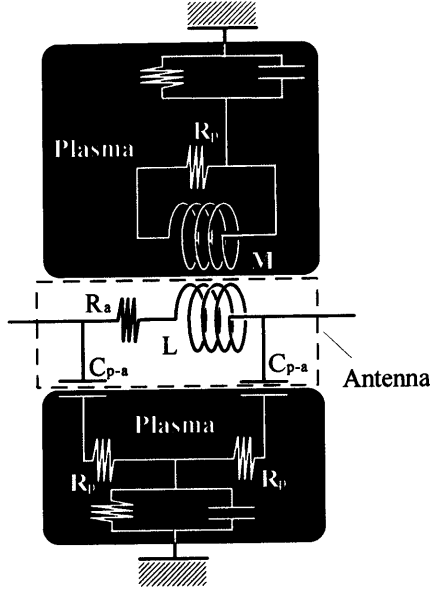
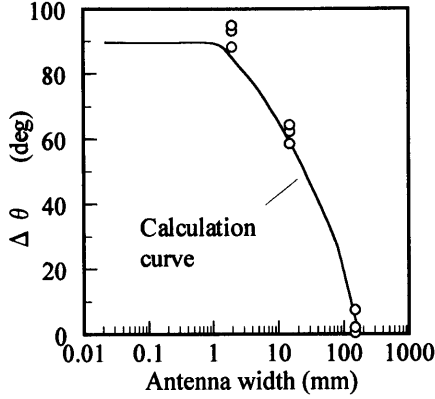**Fig.5** Equivalent circuit model of antenna including plasma [2),3)]

Fig.6 Calculation results of $\Delta\theta_n$ on based of equivalent circuit model [2),3)]

$$Z = \frac{2R_p R_a \gamma + 2R_p \alpha^2 + R_a \beta^2}{(\alpha - \beta)^2 + \gamma^2}$$
$$+ j\frac{-4R_p^2 \alpha - \alpha\beta^2 + \alpha^2\beta + R_a^2\beta}{(\alpha - \beta)^2 + \gamma^2} \qquad (2)$$

where α is $L\omega + M\omega$, β is $(C_1 + C_2)/(C_1 C_2 \omega)$ and γ is $R_a + 2R_p$. $\Delta\theta_n$s can be explained by the calculation based on this model as shown in **Fig.6**. The agreement of the calculation values with the experimental results leads us to the conclusion that $\Delta\theta_n$s is decided by the competition between the inductance and the capacitance. $\Delta\theta_n$ for small C_{p-a} changes grossly as a function of the azimuthal angle from the Load side to the Tune side, for the inductance is not canceled by C_{p-a} at all.
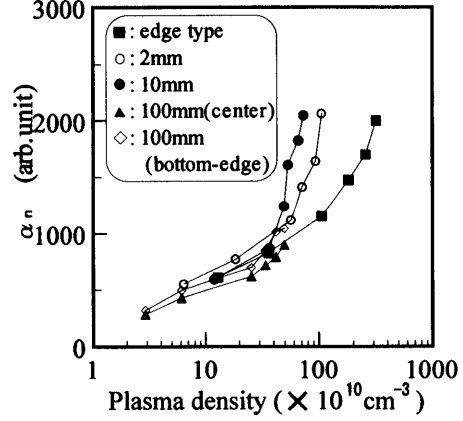

Fig.7 Dependence of extrapolated induction field amplitude at quartz window(α_n) on antenna geometry at 5Pa
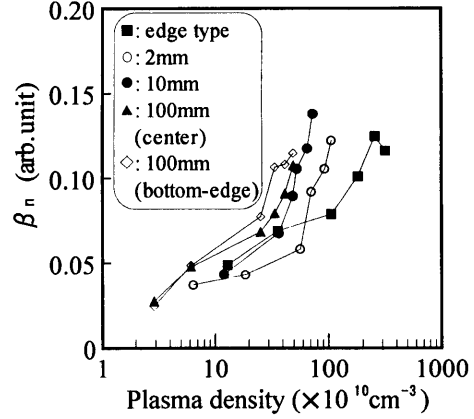

Fig.8 Attenuation coefficient(β_n) dependence on antenna geometry at 5Pa

3.3 Induction Field Measurement

Next, we compared the induction field profiles at the antenna level in Ar plasma at 1Pa, for the induction field induced by the alternative magnetic field is important for an ICP production[4),5)]. Each induction field attenuated exponentially at different rates and was characterized by a curve fitting near the quartz window.

In this paper, the fitting parameters at 5Pa will be shown. Except for the 100mm wide antenna, the extrapolated induction field amplitude at quartz window (α_n) is lower for the antenna with smaller C_{p-a}, as shown in **Fig.7**. But, the attenuation coefficient (β_n) becomes lower for the antenna with smaller C_{p-a} as shown in **Fig.8**. These results indicate that the induction field produced by the antenna with smaller C_{p-a} can penetrate deeply into the plasma irrespective of the pressure.

We verified the electromagnetic field profiles in the plasma by the calculation[4),5)]. We can easily find that the magnetic field profiles are dependent

on the antenna geometry and the calculated profiles agree qualitatively with the experimental results. These results indicate that it is important for the efficient plasma production to penetrate the induction field deeply into the plasma. But, it is worth while examining the subject why the low plasma production is shown for the antenna that produces the strong induction field near the quartz window. The question is taken up later.

On the other hand, at 1Pa, β_{100} at the bottom-edge did not agree with that at the center and was close to β_{10}. Here, we can also realize that the magnetic field produced at the bottom-edges in the 100mm wide antenna can penetrate the magnetic field deeply into the plasma. In this state, the induction current patterns of the 100mm wide antenna are shown in **Fig.9(a),(b)**. (a) is at the bottom-edge level and (b) is at the center level. The triangles indicate the direction of the induction current without the numerical information. At the bottom-edge level, the induction current pattern shows that the induction current circles in the same direction along the antenna in the whole region. The similar induction current patterns are shown at the antenna level of the other antennas. But, the systematic induction current pattern can not be observed near the center level. The maximum magnetic field is produced around the edges and can be penetrated into the plasma, so it is evident that the antenna edge is important to produce the systematic induction current pattern.

3.4 Induction Field Energy

I examined to compare the induction field energies at the antenna level in the plasma at 1Pa[4),5)]. The plasma density is not proportional to the induction field energy (W_{0-63}) in the integral region within 63mm from the quartz window. But, when we ignored the induction field energy near the quartz window, the induction field energy (W_{10-63}) in the integral region over 10mm from the quartz window was proportional to the plasma density irrespective of the antenna.

The results suggest the energy transformation difference near the quartz window with the antenna geometry. The practical energy transformation to the plasma would not be efficient near the quartz window at 1Pa, and the induction field energy penetration into the deep plasma region would be an important factor for the efficient plasma production. **Fig.10** shows the plasma density dependence on W_{0-63} at 5Pa. It is clear that the plasma pro-
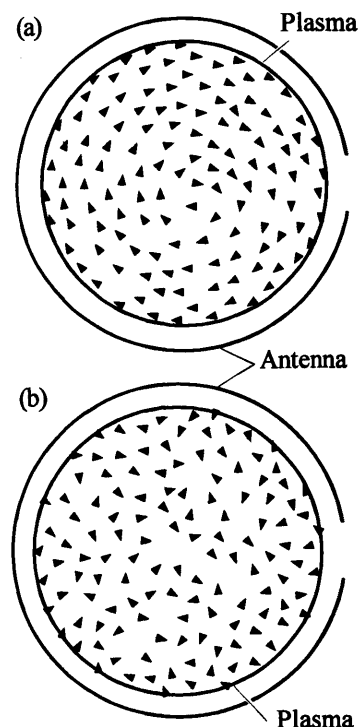

Fig.9 Induction current patterns of the 100mm wide antenna, (a):at bottom-edge level, (b):at center level
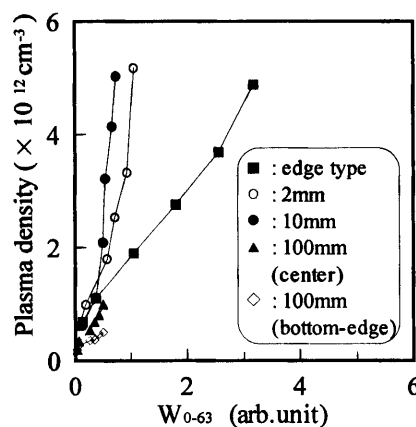

Fig.10 induction field energy (W_{0-63}) dependence on plasma density at 5Pa (Gas:Ar)

duction efficiency depends on the antenna geometry at high plasma density. The plasma production efficiency at 5Pa becomes higher than that at 1Pa at the same energy. We supposed that the heated electron loss at the quartz window would be closely related to the plasma production efficiency and would be given as a function of the geometrical position from the quartz wall. Although the induction energy decreased, the Joule heating is dominant for the energy transformation due to the high collision frequency at 5Pa[6),7)]. On the contrary, the stochas-
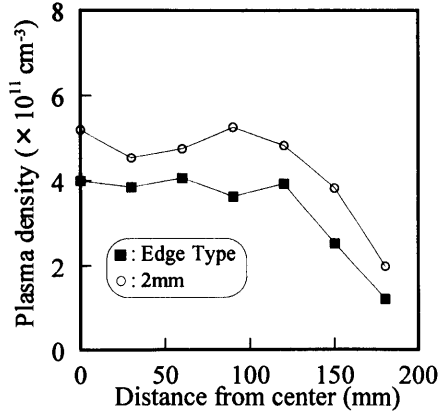
Fig.11 Comparison with plasma densities with and without weak magnetic field (Gas:Ar, Pressure:1.3Pa, Power:1.0kW)
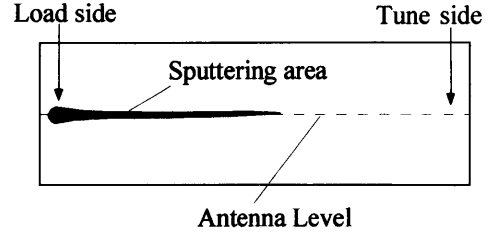

Fig.12 Details diagram of sputtering area on quartz window using 2mm wide antenna

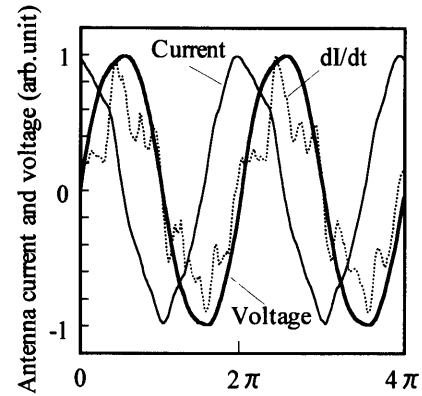

Fig.13 I-V properties at Load side of 150 mm wide antenna (Discharge power: 1000W, Gas: O_2, Pressure: 1.3Pa)

tic heating exists at 1Pa[7], and many heated electrons would extinguish at the quartz window without the induction field energy transformation to the plasma. Therefore, the heated electron would have a higher probability to transform the induction field energy at 5Pa than that at 1Pa. We will discuss this supposition by adding other results in the following.

3.5 DC Magnetic Field Effect

We also improved the plasma uniformity with a magnetic field formed by some permanent magnet rings on the endplate[1),2)]. In this experiment, the plasma uniformity could be improved with ease by the weak magnetic field, in which a magnetic flux was parallel to the quartz window near the quartz window. The plasma uniformity improvement is caused by the plasma loss control at the quartz window. Moreover, we also compared the plasma densities for different types of the antenna in this magnetic field as shown in **Fig.11**. It is evident that the plasma density for the 2mm wide antenna is higher than that of the edge type antenna. Here, it would admit of two interpretations to explain these experiments roughly. One is the extinction of active particles in the bulk plasma, and another is the extinction of the heated electrons near the quartz window.

These antennas showed the almost pure ICP production. In the same magnetic field, it is obvious to consider that the loss probability at the chamber wall does not change on the bulk plasma. Considering the induction energies for these antennas, this result proves clearly that the plasma production efficiency depends on the heated electrons extinction at the quartz window. Therefore, it leads us to the conclusion that the induction field energy near the

quartz window can be transformed efficiently to the plasma due to the suppression of the heated electrons at the quartz window.

Next, the question arises what is the difference between these antennas and the antenna with large C_{p-a} on the plasma production. We will discuss the question in a view point of the quartz window sputtering in the next section.

3.6 Quartz Window Sputtering

We could observe a remarkable quartz window sputtering for the antenna with the C_{p-a} increase, when we used the SiO_2 etching gas at the same discharge power for a long time[1),2)]. The sputtering rate increased remarkably for the antenna with large C_{p-a}. The sputtering rate for the 150mm wide antenna was about 100 times or higher than that of the 2mm wide antenna. Moreover, the spattering area for the 150mm wide antenna corresponded to the whole projected area of the antenna, on the contrary, the sputtering area for the 2mm wide antenna was not symmetric and the sputtering rate was highest at around the feed point of the Load side as shown in **Fig.12**.

As these results, we can say the fairly certainty that the sputtering results in the different mecha-
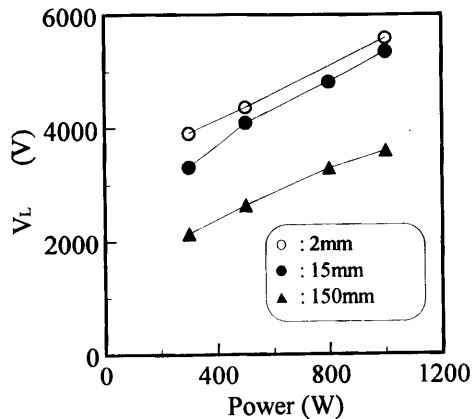
Fig.14 Peak-peak antenna voltage at Load side of each antenna [2],[3]

nism unrelated to the plasma density and needs the mechanism to supply many electrons for the negative sheath formation.

We pays an attention to θ_n, which could be expressed as a function of the azimuthal angle and antenna geometry. θ_{150} at both sides of the antenna was almost 90 degree as shown in **Fig.13**, and does not depend on the antenna position mentioned above. We can point out that the maximum induction field(dashed line) has the same phase of the maximum electric field produced by the antenna voltage. Therefore, the heated electrons would be also accelerated toward the quartz window by the electric field in the whole antenna position. On the other hand, the induction field phase at the Load side of the antenna agree with that of the antenna voltage, but $\Delta\theta_2$ changed as a function of the azimuthal angle by almost 90 degree and the induction field phase does not agree with the antenna voltage phase at the Tune side. The sputtering area shown in **Fig.12** corresponds to the antenna position with the phase, which the induction field is close to the phase of the antenna voltage.

Moreover, we consider the capacitance between antenna and the plasma, too. The peak-peak antenna voltage at the Load side is shown in **Fig.14**. The sputtering rate is not proportional to the antenna voltage. The result indicates that the antenna with large C_{p-a} coupled strongly with the plasma due to a low impedance to the plasma and would enhance the more electron loss.

We finally summarized that the sputtering arises from the synergism of the following factors. One is the phase effect between the induction field and the antenna voltage, and another is the capacitively coupling.

4. Conclusion

In ICP, it is important how to control the loss of the heated electrons at the quartz wall, which play an important role to transport the induction field energy to the plasma. To raise the plasma production efficiency, we may go from these experimental results to the following conclusion.

Firstly, the heated electron loss at the quartz window would decrease by the induction field penetration deeply into the plasma, for the loss probability decreased as a function of the distance from the quartz window. Otherwise, we should apply a weak magnetic field to drop the electron loss probability at the quartz window as mentioned in this paper.

Secondly, we should never make the phase of antenna voltage agree with that of the induction field throughout the antenna, to prevent the heated electron from accelerating toward the quartz window by the electric field due to a capacitive coupling between the plasma and the antenna. However, the electric field did not depend on the maximum antenna voltage but on C_{p-a}. Therefore, it is the most reasonable method that we apply the antenna with the minimum C_{p-a} to control the electron loss

5. Acknowledgements

References

1) K. Takagi; Y. Nakagawa; T, Tsukada: Tech. Rep. ANELVA. Corp. **1-3** (1996)25. (in Japanese)
2) K. Takagi; Y. Nakagawa; T, Tsukada: *Proc. 189th. ECS meeting(Los Angels).* **96-12** (1996)116.
3) K. Takagi: *US-PATENT 5681393.*
4) K. Takagi; K. Iwatani; Y. Kuroki: *Research. Report. ISEE. Kyushu University.* **4-2** (1999)139.
5) K. Takagi; K. Iwatani; Y. Kuroki: *Proc. 199th. ECS meeting(Hawaii).* in publishing
6) V. A. Godyak; R. B. Piejack; B. M. Alexandravich; V. I. Kolobof: *Phys. Rev. Letter.* **80** (1998)3264.
7) M. Turner; *Phys. Rev. Let.* **71** (1993)1844.